How to combine reflection and transmission THz-TDS measurements to get precise extraction of complex refractive index ....

Data · September 2015

CITATIONS
0

READS
166

3 authors, including:

Maxime Bernier
Université Savoie Mont Blanc
44 PUBLICATIONS **144** CITATIONS
SEE PROFILE

Frederic Garet
Université Savoie Mont Blanc
171 PUBLICATIONS **1,756** CITATIONS
SEE PROFILE

Precise Determination of the Refractive Index of Samples Showing Low Transmission Bands by THz Time-Domain Spectroscopy

Maxime Bernier, Frédéric Garet, and Jean-Louis Coutaz

***Abstract*—In this paper, we propose a method to determine the refractive index and the absorption coefficient of samples showing spectral bands of very low transmission. The method, takes advantages of both transmission and reflection terahertz time-domain spectroscopy (THz-TDS) to obtain more precise optical constants than when only reflection measurement is used. It has been then validated using pellets made of maltose, which exhibits resonant lines within the THz spectral range.**

***Index Terms*—Material characterization, reflection spectroscopy, transmission spectroscopy, THz time-domain spectroscopy (THz-TDS).**

I. Introduction

SAMPLES may exhibit a very low transmission in some narrow spectral bands due to a strong absorption by the sample material or to some electromagnetic resonance effects in the sample. In the terahertz (THz) domain, the first case corresponds mostly to the excitation of phonons or/and of molecular resonances (roto-vibrations). The second case is encountered when the sample can support electromagnetic modes (Fabry–Pérot-like oscillations, photonic band gaps, guided modes, etc.). Inside these bands, the amplitude of the transmitted THz signal tends to 0 and its phase cannot be measured while, outside the bands, the signal is strong enough to be detected. Thus classical transmission THz time-domain spectroscopy (THz-TDS) [1], based on the knowledge of both modulus and phase of coefficient of transmission, does not permit to extract the refractive index and the absorption coefficient over the whole THz spectral range since the lack of signal in the first low transmission band involves a loss of the phase reference. A way to overcome this problem is to employ very thin samples, with thicknesses of the order of μm's or even thinner, through which THz waves are transmitted even if absorption is huge. However, for several materials like powders or liquids, fabrication of thin samples is not possible. Such materials can be also characterized by reflection THz-TDS [2] but with a weaker precision [3]. Indeed, the phase of the reflected signal is only given by the Fresnel reflection coefficient, and is much smaller than the one measured in transmission, which results from the propagation through the whole thickness of the sample. Thus, material parameters extracted from reflection THz-TDS measurement are less precise. In addition, reflection THz-TDS is very sensitive to any shift in the relative location of the sample as compared to a reference mirror [4], leading to less accurate characterization. In this paper, a method dedicated to the precise characterization of material presenting low-transmission bands is proposed. This automated extraction technique is based on combined reflection and transmission THz-TDS (R&T THz-TDS) measurements, and has been experimentally validated with maltose pellets [5].

Manuscript received November 05, 2012; revised February 06, 2013; accepted February 13, 2013. Date of publication March 11, 2013; date of current version April 29, 2013.

The authors are with the IMEP-LAHC, UMR C.N.R.S. 5130, University of Savoie, 73 376 Le Bourget du Lac Cedex, France (e-mail: maxime.bernier@univ-savoie.fr; frederic.gare@univ-savoie.fr; jean-louis.coutaz@univ-savoie.fr).

Color versions of one or more of the figures in this paper are available online at http://ieeexplore.ieee.org.

Digital Object Identifier 10.1109/TTHZ.2013.2247793

II. Principle of the Method

A. General Considerations on Transmission THz-TDS

In classical transmission THz-TDS [6], the sample is illuminated under normal incidence by a waveform delivered by the emitting antenna excited by a femtosecond pulse train and the transmitted signal is temporally sampled at the receiving antenna. Usually, the sample is a slab of homogeneous material with flat parallel faces. The sample is located in a region of the THz-TDS set up where the beam is parallel or could be considered as parallel (at the waist of a focusing optics with a Rayleigh length much bigger than the sample thickness). The measured complex coefficient $\tilde{T}_{\rm meas}(\omega)$ of the sample is obtained by taking the ratio of the Fourier-transformed waveforms $\tilde{S}_{T,\rm samp}$ with and $\tilde{S}_{T,\rm ref}$ without the sample in the THz beam

$$\tilde{T}_{\rm meas}(\omega) = \frac{\tilde{S}_{T,\rm samp}(\omega)}{\tilde{S}_{T,ref}(\omega)} = T_{\rm meas}(\omega)\ e^{j\,\phi_T(\omega)} \tag{1}$$

where ω is the angular frequency, $T_{\rm meas}(\omega)$ and $\phi_T(\omega)$ are, respectively, the modulus and phase of $\tilde{T}_{\rm meas}(\omega)$. For sake of simplicity, we will not write the ω-dependence of the variables from now on. For a homogeneous slab with parallel faces, the expression of the transmission coefficient $\tilde{T}$ is known, from electromagnetism theory, and writes

$$\tilde{T} = 4\tilde{n}\,n_o \frac{1-\left(\frac{\tilde{n}-n_o}{\tilde{n}+n_o}\right)^{2(N+1)} e^{-j2\omega/c\tilde{n}\,(N+1)d}}{(\tilde{n}+n_o)^2-(\tilde{n}-n_o)^2\ e^{-j2\omega/c\tilde{n}\,d}} \times e^{-j\omega d/c(\tilde{n}-n_o)} \tag{2}$$

$\tilde{n} = n - j\kappa$ is the complex refractive index of the sample, d is its thickness, c is the speed of light in vacuum and n_o is the refractive index of the surrounding medium (usually air or vacuum). N is the number of back and forth reflections of the THz waveform in the sample. Ideally, N tends towards infinity and expression (2) becomes:

$$\tilde{T} = \frac{4\tilde{n}\, n_o e^{-j\omega d/c(\tilde{n}-n_o)}}{(\tilde{n}+n_o)^2 - (\tilde{n}-n_o)^2\ e^{-j2\omega/c\tilde{n}\, d}}. \tag{3}$$

In actual experiments, N is limited to a finite number by the length of the delay line used for recording the temporal signals. On the other hand, in the case of thick enough samples, only the waveform directly transmitted ($N = 0$) by the sample can be saved and all the rebounds are rejected by an appropriate time-windowing. Expression (2) simplifies into:

$$\tilde{T} = \frac{4\tilde{n}\, n_o}{(\tilde{n}+n_o)^2} e^{-j\omega d/c(\tilde{n}-n_o)}. \tag{4}$$

Let us notice that the $N = 0$ simplification is done to the detriment of both spectral resolution and precision of the extraction [6].

The refractive index of the sample extracted from transmission measurements, noted $\tilde{n}_T = n_T - j\kappa_T$, is obtained by solving the equation $\tilde{T}_{\text{meas}} = \tilde{T}$ using either expression (2), (3) or (4), depending on the considered experimental case. Because of the involved complex values and of the oscillatory behavior of $\tilde{T}$, the extraction is performed numerically and can be very fast using smart extraction procedures [6], [8]–[10]. The extraction requires the knowledge of both experimental modulus and phase. Fourier-transform codes give the phase of the signal within a π-range. Thus, the phase should be unwrapped and, as no signal is measured at low frequencies in THz-TDS setups, it is usually taken to be null at $\omega = 0$ and linearly extrapolated up to the first relevant value. When samples show strong absorption bands, i.e., the transmitted signal is below the noise threshold, the phase cannot be known within these bands. Moreover, for higher frequencies, the unwrapping process is no more possible and thus the so-determined phase ϕ_T differs by an amount $2m\pi$, where m is an unknown integer, from the actual phase ϕ_{To}

$$\phi_T = \phi_{To} + 2m\pi. \tag{5}$$

B. General Considerations on Reflection THz-TDS

In reflection configuration under a normal incidence, the incoming THz wave is reflected at the surface of the tested sample without propagating through the absorbing material, unless inner reflections are taken into account. For sufficiently thick absorbing samples, this hypothesis is fulfilled. If this is not the case, temporal rebounds may be erased by an appropriate time-windowing, as explained for the transmission case. Thus, the complex reflection coefficient $\tilde{R}$ is simply the Fresnel reflection coefficient:

$$\tilde{R}_{\text{meas}} = \frac{\tilde{S}_{R,\text{samp}}}{\tilde{S}_{R,ref}} = R_{\text{meas}}\, e^{j\phi_R} = \tilde{R} = \frac{\tilde{n}_R - 1}{\tilde{n}_R + 1}. \tag{6}$$

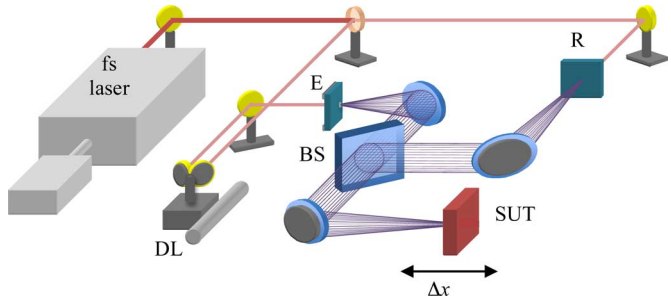

Fig. 1. THz-TDS setup in reflection in normal incidence configuration (DL = delay line, SUT = sample under test, PM = parabolic mirror, E = THz emitter, R = THz receiver, BS = beam splitter).

Here, the reference signal $\tilde{S}_{R,ref}$ is obtained by using a metallic mirror instead of the sample, which is assumed to be a perfect reflector.

The value of the refractive index $\tilde{n}_R = n_R - j\,\kappa_R$ extracted from reflection measurement is directly calculated by inverting expression (6)

$$\begin{cases} n_R = \frac{1-R^2_{\text{meas}}}{1+R^2_{\text{meas}}-2R_{\text{meas}}\cos\phi_R} \\ \kappa_R = -\frac{2R_{\text{meas}}\sin\phi_R}{1+R^2_{\text{meas}}-2R_{\text{meas}}\cos\phi_R}. \end{cases} \tag{7}$$

The main drawback of reflection measurements is related to the error induced by an even small misalignment Δx of the reference mirror as compared to the position of the sample (see Fig. 1). This induces a phase error:

$$\Delta\phi = \frac{2\Delta x\omega}{c} \tag{8}$$

and thus errors on the extracted value of the refractive index

$$\begin{cases} \frac{\Delta n_R}{n_R} \approx \kappa_R \Delta\phi = \frac{2\omega\,\kappa_R}{c}\,\Delta x = \alpha_R\,\Delta x \\ \frac{\Delta\kappa_R}{\kappa_R} \approx abs\left[\frac{\alpha_R}{2} - \frac{2\omega^2\left(n_R^2-1\right)}{c^2\,\alpha_R}\right]\Delta x \end{cases} \tag{9}$$

where $\alpha_R = 2\omega\,\kappa_R/c$ is the coefficient of absorption of the material. Regarding (9), the relative errors made on the real and imaginary parts of the complex refractive index be have differently when the material is getting more and more absorbing. Indeed, the error induced on n_R by the misalignment Δx is getting bigger when α_R increases, whereas the error made on κ_R decreases until the absorption coefficient reaches $2\omega\,\sqrt{n_R^2-1}/c$. Above this latter value, which ranges from tens to hundreds of cm^{-1} in the THz range, $\Delta\kappa_R/\kappa_R$ gets bigger with increasing α_R.

Therefore, for a highly absorbing material, the uncertainties made on the optical properties of the tested sample are quite big and deserve to be corrected either by numerical [11] or experimental [12] solutions. Nevertheless, even if this technique is weakly precise, it allows one to estimate the refractive index of the absorbing material even in spectral regions where absorption is huge.

C. Combined Transmission-Reflection Method

As explained above, for samples exhibiting a strong absorption in some given spectral regions, the phase ϕ_T of the transmitted signal is lost, and thus a correct extraction of the material parameters is not possible for frequencies higher than ones

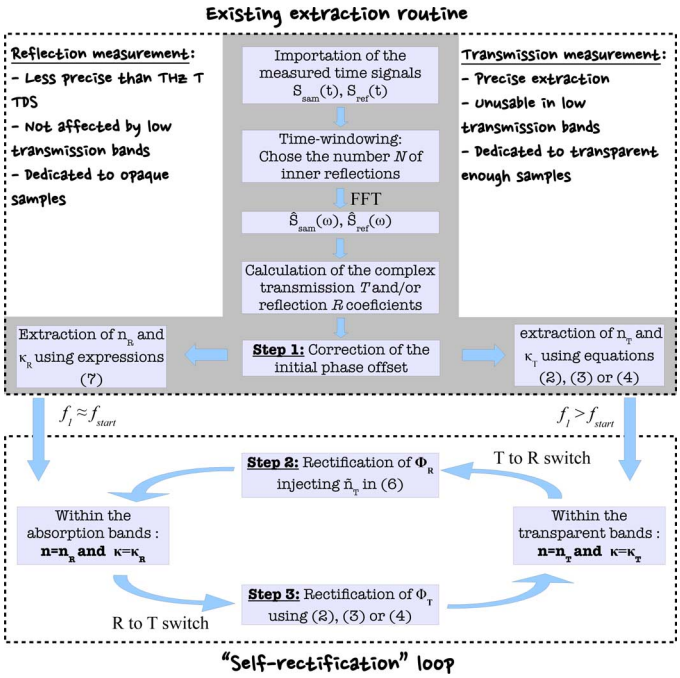

Fig. 2. Block diagram summarizing the extraction process based on the combined R&T THz-TDS method.

of the first low transmission band. When using a reflection technique instead, the precision on the extraction is strongly affected by an error on the measured phase ϕ_R of the reflected signal due to some misalignment of the reference mirror as compared to the sample position. Here, we present a method, which allows one both to retrieve the phase in transmission in all the regions of sample transparency, and to correct the phase from misalignment errors in the case of reflection. As in any THz-TDS study, our method gives accurate values of the refractive index only if the material does not exhibit strong absorption bands below the smallest reachable THz frequency f_{start}, usually below 0.1 THz, i.e., in the radio-frequency domain.

Let us consider a transparent sample presenting a first low transmission band, which spreads from f_1 to f_2. We suppose that the lower frequency f_1 is larger than f_{start}. In the range $f_{\text{start}} - f_1$, the sample is transparent and thus we perform a study in transmission, which leads to an accurate value of $\tilde{n}_T$, assuming a linear extrapolation of the phase towards $f = 0$, as explained above and presented in Fig. 2 (see step 1), which is permitted thanks to the absence of absorption band below f_{start}. Then $\tilde{n}_R$ is correctly extracted from reflection data over the whole reachable THz band. Indeed, by making $\tilde{n}_R = \tilde{n}_T = \tilde{n}$ in the $f_{\text{start}} - f_1$ range, we determine the phase error $\Delta\phi = 2\Delta x\omega/c$ (relation (8)) in the reflection data and thus the misalignment Δx. We then can correct it over the whole THz range (see step 2 in Fig. 2).

In the first absorption band $f_1 - f_2$, only the previously corrected $\tilde{n}_R$ is determined, and so we set $\tilde{n} = \tilde{n}_R$. For frequencies higher than f_2 up to the next absorption band if any, the sample is again sufficiently transparent to be accurately characterized in transmission. However, in this spectral range, the experimentally determined phase in transmission ϕ_T could differ from the actual value ϕ_{To} by a $2m\pi$ amount (relation (5)). This unknown $2m\pi$ value is resolved as follows (see step 3 in Fig. 2): in fact, $\tilde{n}_R$ is known from the reflection measurement and we calculate the phase in transmission $\phi_{To,\text{calc}}$ from this value using either (2), (3) or (4). By comparing ϕ_T and $\phi_{To,\text{calc}}$, we find $2m\pi$. Thus, the classical parameter extraction procedure in transmission is employed to derive $\tilde{n}_T$. As this value is obtained with a great accuracy, we set $\tilde{n} = \tilde{n}_T$. If the sample exhibits additional absorption bands, the same procedure, we call "self-rectification loop", is repeated for each band (see Fig. 2).

This R&T THz-TDS method requires at least two measurements (i.e., in transmission and in reflection) to get the value of $\tilde{n}$ over the whole studied THz domain. In the regions of transparency, $\tilde{n}$ is determined with a great accuracy thanks to transmission measurement. In the absorption bands, $\tilde{n}$ is derived from corrected reflection data, its value is less accurate but still measurable. The frequency point at which one switches from transmission to reflection measurements (and vice-versa), is selected as follows. As one approaches to low-transmission bands, the transmitted THz signal gets noisier, in opposite to the reflected one. Thus, as soon as the standard deviation of a set of transmission data becomes bigger than the one calculated from a set of reflection measurements, one switches to reflection extraction. Asymmetrical procedure is employed to define the upper frequency of the low-transmission band at which one switches from reflection to transmission measurements.

The phase retrieval implies that the sample material response does not show spectral features that induce transmission phase jumps larger than π between two consecutive frequency values of the recorded spectrum. Otherwise, the extraction code will mix up π-phase jumps due to the material, on the one hand, and given by the Fourier transform, on the other hand. Getting the spectra with a better spectral resolution, which is achieved enlarging the recorded temporal window, could solve this problem. As in classical THz-TDS, it is supposed that the material does not exhibit strong absorption peaks in the radio-frequency region.

III. Experimental Validation

The R&T THz-TDS procedure is validated with a classical homemade THz-TDS, which can be configured either in transmission or in reflection geometry scheme. The THz waveforms are delivered and detected with photo-conducting LTG-GaAs antennas. The available THz spectrum reaches 5 THz, which permits, in the present study, data extraction in the range 0.1–2.1 THz with typically a 60-dB dynamic range. In both configurations, the sample under test is placed at the focal point of an off-axis parabolic mirror, where the focalized THz Gaussian beam presents a waist of 1.06 mm (measured at 600 GHz). In the reflection configuration, the THz signal back reflected from the surface of the sample is collected using a 1-cm thick high resistivity silicon slab as a beam splitter (see Fig. 1).

Maltose is chosen as case-study material since it exhibits strong absorption lines in the THz range involved by low frequency vibrational modes. As the maltose is of great interest for security and pharmacological applications, its properties have been characterized by several teams using either THz-TDS [13]–[17] or FTIR spectroscopy [18]. This provides accurate

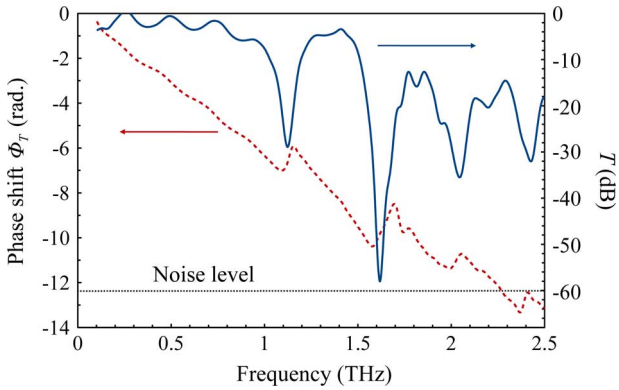

Fig. 3. Measured modulus (solid line) and phase (dashed line) of the transmission coefficient $\bar{T}$ of a 325-μm thick maltose pellet.

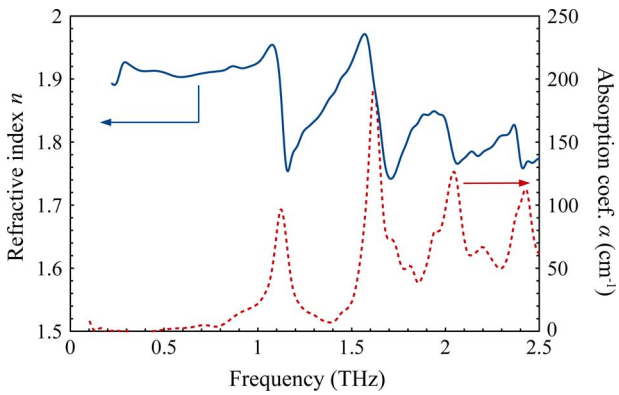

Fig. 4. Refractive index n and absorption coefficient α extracted from the transmission data shown in Fig. 3.

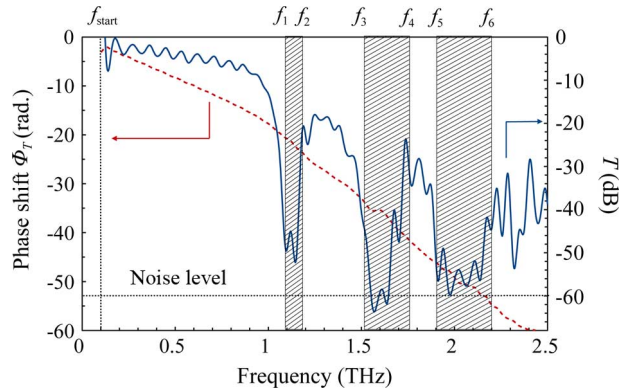

Fig. 5. Measured modulus (solid line) and phase (dashed line) of the transmission coefficient $\bar{T}$ of a 890-μm thick maltose pellet. The hatched areas correspond to the strong absorption bands.

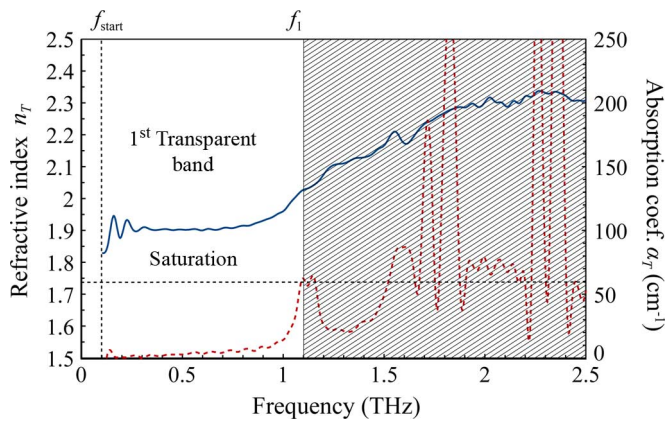

Fig. 6. Refractive index n_T and absorption coefficient α_T extracted from the transmission data shown in Fig. 5. In the hatched area, i.e., over the first absorption band, extracted values are erroneous because the absolute phase of the transmitted signal is not known.

THz response database[1], which can either validate or discriminate results of the present study. Moreover, maltose powder can be pressed to form pellets of desired thickness whose grains size is much smaller than the THz wavelength, making negligible THz wave scattering [16], [19].

The maltose pellets (13-mm diameter) have been made by pressing a pure maltose monohydrate (90%) powder, purchased from Arcos Organics (Lot A0293726), in a mechanical press under 5-tons/cm^2 pressure. Two pellets of different thickness have been produced from the same powder and using the same fabrication recipe. These pellets have been then immediately stored in a same Petri dish filled with silica gel to avoid any humidity issue. The first one is 325-μm thick: even in the absorption regions, the transmitted signal is strong enough to be detected (see Fig. 3). Its thickness has been first estimated with a caliper and then determined by minimizing the oscillations of the extracted refractive index curve. As explained in [7], this leads to a very precise value of $d = 325 \pm 2$ μm. As this sample is thin enough, $\tilde{n}$ is accurately extracted over the whole THz range using only transmission data (Fig. 4), and serves as reference value to experimentally check the validity of our method.

The second sample is 890-μm thick. In the region of strong absorption, the signal transmitted by this sample is below the noise level of the setup (Fig. 5) and thus our combined R&T THz-TDS method is necessary to extract $\tilde{n}$ over the whole 0.1–2.1 THz range.

Indeed, if a classical THz-TDS extraction is performed without phase correction, the loss of the absolute phase in the absorption region leads in turn to a saturation of the absorption coefficient within each absorption band, and simultaneously to a vertical shift of the refractive index over the whole bandwidth following the first absorption band, as shown in Fig. 6. Following the procedure described in Section II-C, we first extract $\tilde{n}_T$ from transmission data up to $f_1 \approx 1.1$ THz and then we extract $\tilde{n}_R$ over the whole range 0.1–2.5 THz. By adjusting the phase error $\Delta\phi = 2\Delta x\omega/c$, we force $\tilde{n}_R$ to be equal to $\tilde{n}_T$ over the range $f_{\text{start}} - f_1$. Fig. 7 shows the phase in reflection ϕ_R as measured (dashed line) and as calculated from the known value $\tilde{n}_T$.

The inset shows the difference between the measured and calculated phases, which is fitted by a straight line leading to the Δx value. Here, the best agreement is obtained for $\Delta x = 5$ μm. Then, the phase in reflection is corrected over the whole THz range and the corrected data are used to extract $\tilde{n}_R$ as presented

[1]http://webbook.nist.gov; http://thzdb.org

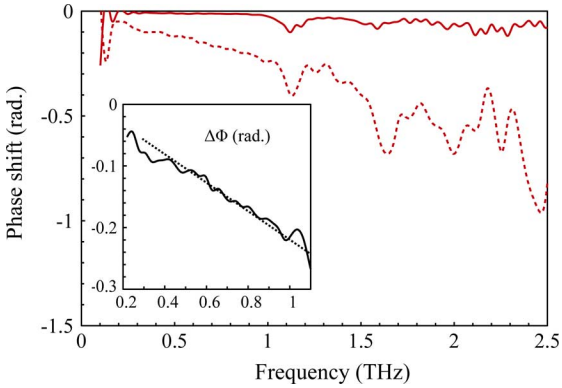

Fig. 7. ϕ_R vs frequency as measured in reflection (dashed line) and calculated (solid line) with the value $\tilde{n}_T$ extracted form the transmission data (Fig. 6). Inset: Difference between the 2 phases (solid line) versus frequency. The linear plot (dashed line) allows us to determine the sample misplacement relatively to the reference mirror position.

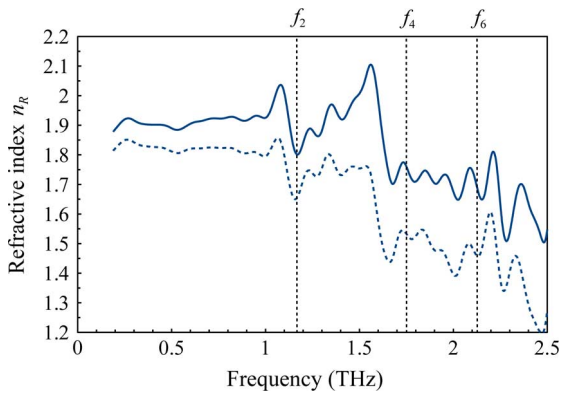

Fig. 8. Refractive index n_R vs frequency extracted from reflection data: phase-corrected value (solid line) and uncorrected value (dashed line).

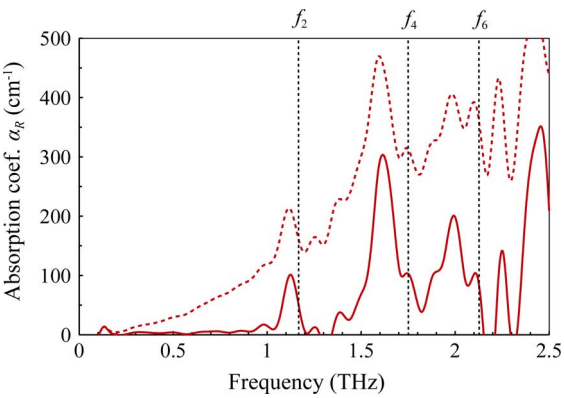

Fig. 9. Absorption coefficient α_R vs frequency extracted from reflection data: phase-corrected value (solid line) and uncorrected value (dashed line).

in Figs. 8 and 9. To show the effect of the misalignment, the uncorrected values are also plotted on the same figure.

Typically, the refractive index n is underestimated by $20\% \sim 30\%$, while the absorption is strongly overestimated, especially in the regions of transparency. To get a better (than $\tilde{n}_R$) estimation of $\tilde{n}$ in the regions of transparency, the transmission data are considered. Because of the lack of signal in the absorption bands, the experimental phase ϕ_T exhibits $2m\pi$ phase jumps (m being an integer) randomly induced by each absorption band,

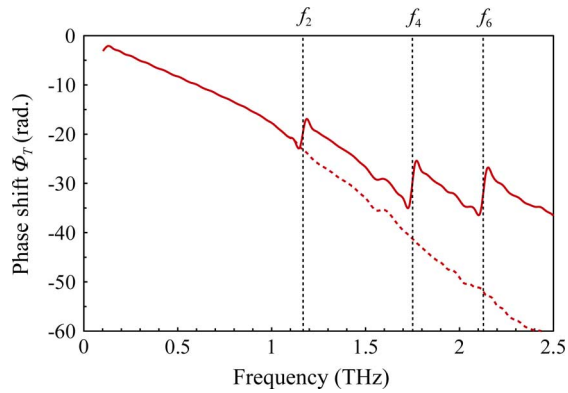

Fig. 10. Experimental phase spectrum of the coefficient of transmission: uncorrected plot (dashed line), corrected plot (solid line).

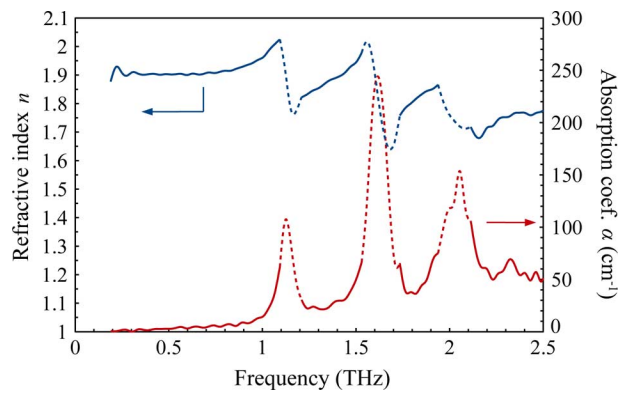

Fig. 11. Refractive index (blue line) and absorption coefficient (red line) of maltose vs frequency. The solid lines are obtained from transmission data while the dashed lines are determined from reflection data.

as seen in Fig. 10. As explained previously, we get the actual values of m by comparing the experimental phase ϕ_T with the one calculated from relation (2), (3), or (4), where the value of $\tilde{n}_R$, measured in reflection, is considered.

The corrected phase ϕ_{T0} is plotted as a dashed line in Fig. 10, and the jump artifacts have been removed. From this corrected phase, the accurate value of $\tilde{n}_T$ can be extracted in the regions of transparency. Therefore, taken $\tilde{n} = \tilde{n}_T$ in the regions of transparency and $\tilde{n} = \tilde{n}_R$ in the absorption bands allows us to accurately determine $\tilde{n}$ over the whole studied THz domain. The results are shown in Fig. 11.

As compared to the curves obtained in reflection THz-TDS (Figs. 8 and 9), the ones achieved through this combined method are definitively less noisy and more defined. Some oscillation features, due to noise, observed in Figs. 8 and 9, have been removed and thus the absorption peaks centered at 1.12, 1.62 and 2.05 THz are clearly observed. These values are in very good agreement with the data published in the literature . In between these peaks, absorption increases exponentially with frequency, which could be interpreted as a residual scattering effect (the so-called Christiansen effect [20]) by the grains of the powder [16], [19]. The refractive index is almost constant in spectral ranges far from the absorption frequencies. For each absorption band, the refractive index curve exhibits a typical resonant feature. Because of these features, the overall variation of the refractive index with frequency is basically decreasing.

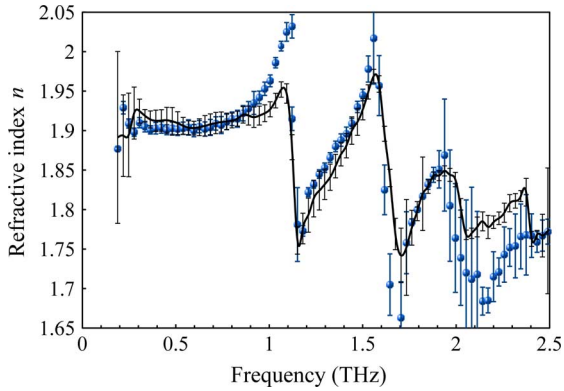

Fig. 12. Refractive index vs frequency of the 890-μm thick sample extracted using the combined THz-TDS method (dots), and of the 325-μm thick reference sample (solid line) extracted using classical transmission THz-TDS.

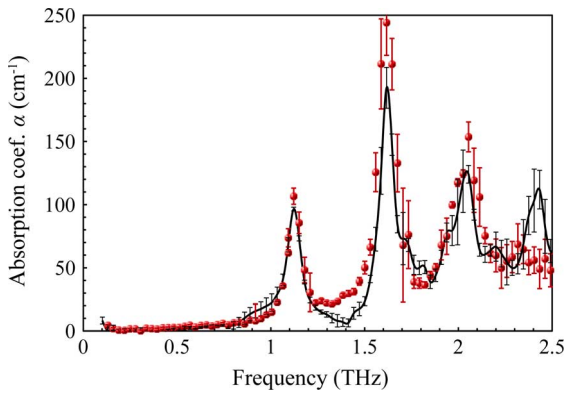

Fig. 13. Absorption vs frequency of the 890-μm thick sample extracted using the combined THz-TDS method (dots), and of the 325-μm thick reference sample (solid line) extracted using classical transmission THz-TDS.

The weakness of the THz signal delivered by the photo-conducting antenna, in addition to the lack of the setup sensitivity at higher frequencies, lead to noisy curves above 2.2 THz. This involves inaccurate extraction of $\tilde{n}$ at these frequencies, as shown in Fig. 12.

Finally, the method validated by comparing the data shown on Fig. 11, with the values achieved with the 325-μm thick reference sample. Figs. 12 and 13 present spectra of the refractive index n of maltose extracted with the combined method for the 890-μm thick reference sample and with the classical method for 325-μm thick sample. The error bars for the combined method data correspond to the standard deviation obtained from a set of 10 measurements. They do not include any systematic error.

The refractive index obtained with the combined method is in good agreement with the one achieved with the thinner sample and a classical THz-TDS method in transmission. Of course, this latter method is more accurate than the combined one, but we recall the reader that it cannot be applied for thick samples (see Fig. 6). The main differences between both determinations are seen around each resonance, for example at $\sim$ 1.1 THz, and above 2.1 THz. At each resonance, i.e in the absorption bands, the refractive index is extracted from reflection data and, as explained previously, the measurement in reflection is less accurate (error due to noise) and more sensitive to any misalignment of the sample (systematic shift) than in transmission, leading to larger uncertainties within these absorption bands. The systematic shift leads to an overestimation of both the real part of the index and of the absorption, which cannot be corrected by averaging several curves, as it is done for the effect of noise. At higher frequencies, the weakness of signals transmitted and reflected by the 890-ìm thick sample makes the results very sensitive to noise. Over 2.1 THz, the SNR on the reflection measurements is too poor to use the combined method, and the presented optical parameters are extracted only from the noisy transmission measurements. Thus, the known peak at 2.41 THz is not resolved with the combined method (see Fig. 13). Moreover, as the transmitted phase cannot be corrected over 2.1 THz, the refractive index is shifted (see Fig. 12).

The combined method gives results close the ones achieved with the thinner sample in transmission THz-TDS. Above 2.1 THz, the combined method is less precise and accurate due to noise.

IV. Conclusion

In this paper, we have proposed and experimentally demonstrated the principle of a combined reflection-transmission THz-TDS method. This technique makes it possible to determine the refractive index and absorption coefficient of a sample over the entire accessible frequency range, even when the sample spectrum contains strong absorption bands for which almost no THz signal is transmitted. The basic idea of the method is to correct, by comparison between reflection and transmission data, the error on the reflected phase due to a misplacement of the reference mirror, and the π-jump phase errors in transmission that originate in the lack of transmitted signal in the absorption bands. Here the method is validated with maltose pellets, whose absorption peaks are related to the excitation of low frequency vibration modes of the maltose molecule. For such samples, our method is better (see Fig. 11) than transmission THz-TDS (see Fig. 6) extraction, as this latter is not valid over the first absorption band, and is more precise than reflection THz-TDS (see Figs. 8 and 9) extraction, even if misalignment-induced shifts have been corrected. Indeed, reflection THz-TDS suffers from a lack of reflected signal over the whole THz range, leading to less precise characterization. On the contrary, in our combined method, the signal in the regions of transparency is strong and allows a nice correction of the determined parameters. This combined reflection-transmission THz-TDS extraction method has been applied to crystals that exhibit strong phonon lines, like superionic semiconductors [21], and could hopefully be used to investigate samples presenting electromagnetic resonances like Fabry–Pérot modes, guided modes, or photonic bandgaps.

Acknowledgment

The authors would like to thank Dr. S. Joly, a former post-doctorate fellow at the IMEP-LAHC laboratory, for advising us in fabricating the maltose pellets.

References

[1] , D. M. Mittleman, Ed., *Sensing With Terahertz Radiation*. New York, NY, USA: Springer-Verlag, 2003.

[2] L. Thrane, R. H. Jacobsen, P. U. Jepsen, and S. R. Keiding, "THz reflection spectroscopy of liquid water," *Chem. Phys. Lett.*, vol. 240, no. 4, pp. 330–333, Jun. 1995.
[3] P. U. Jepsen and B. M. Fisher, "Dynamic range in terahertz time-domain transmission and reflection spectroscopy," *Opt. Lett.*, vol. 30, no. 1, pp. 29–31, Jan. 2005.
[4] A. Pashkin, M. Kempa, H. Nemec, F. Kaldec, and P. Kuzel, "Phase-sensitive time-domain terahertz reflection spectroscopy," *Rev. Sci. Instrum.*, vol. 74, no. 11, pp. 4771–4777, Nov. 2003.
[5] M. Bernier, F. Garet, R. Sardarly, and J.-L. Coutaz, "Precise determination of the complex refractive index of samples showing low transmission bands by THz time-domain spectroscopy," in *Topical Meeting on THz Sci. and Technol. Eur. Opt. Soc.*, Prague, Czech Republic, Jun. 17–20, 2012.
[6] L. Duvillaret, F. Garet, and J.-L. Coutaz, "A reliable method for extraction of material parameters in terahertz time-domain spectroscopy," *IEEE J. Sel. Topics Quantum Electron.*, vol. 2, no. 3, pp. 739–746, Sep./Oct. 1996.
[7] L. Duvillaret, F. Garet, and J.-L. Coutaz, "Highly precise determination of optical constants and sample thickness in terahertz time-domain spectroscopy," *Appl. Opt.*, vol. 38, no. 2, pp. 409–415, 1999.
[8] M. Scheller, C. Jansen, and M. Koch, "Analyzing sub-100-μm samples with transmission terahertz time domain spectroscopy," *Opt. Commun.*, vol. 282, no. 7, pp. 1304–1306, Apr. 2009.
[9] I. Pupeza, R. Wilk, and M. Koch, "Highly accurate optical material parameter determination with THz time-domain spectroscopy," *Opt. Express*, vol. 15, no. 7, pp. 4335–4350, Apr. 2007.
[10] T. D. Dorney, R. G. Baraniuk, and D. M. Mittleman, "Material parameter estimation with terahertz time-domain spectroscopy," *J. Opt. Soc. Amer. A*, vol. 18, no. 7, pp. 1562–1571, Jul. 2001.
[11] M. Khazan, R. Meissner, and I. Wilke, "Convertible transmission-reflection time-domain terahertz spectroscopy," *Rev. Sci. Instrum.*, vol. 72, no. 8, pp. 3424–3430, Aug. 2001.
[12] E. M. Vartiainen, Y. Ino, R. Shimano, M. Kuwata-Gonokami, Y. P. Svirko, and K.-E. Peiponen, "Numerical phase correction method for terahertz time-domain reflection spectroscopy," *J. Appl. Phys.*, vol. 96, pp. 4171–4176, Jun. 2004.
[13] Y. C. Shen, P. C. Upadhya, H. E. Beere, E. H. Linfield, A. G. Davies, I. S. Gregory, C. Baker, W. R. Tribe, and M. J. Evans, "Generation and detection of ultrabroadband terahertz radiation using photoconductive emitters and receivers," *Appl. Phys. Lett.*, vol. 85, no. 2, pp. 164–166, Jul. 2004.
[14] P. C. Upadhya, Y. C. Shen, A. G. Davies, and E. H. Linfield, "Far-infrared vibrational modes of polycrystalline saccharides," *Vib. Spectrosc.*, vol. 35, no. 1, pp. 139–143, Jun. 2004.
[15] E. R. Brown, J. E. Bjarnason, A. M. Fedor, and T. M. Korter, "On the strong and narrow absorption signature in lactose at 0.53 THz," *Appl. Phys. Lett.*, vol. 90, no. 6, pp. 061908–061908, Feb. 2007.
[16] M. Franz, B. M. Fisher, and M. Walther, "The Christiansen effect in terahertz time-domain spectra of coarse-grained powders," *Appl. Phys. Lett.*, vol. 92, no. 2, pp. 021107–021107, Jan. 2008.
[17] A. Nakanishi, Y. Kawada, T. Yasuda, K. Akiyama, and H. Takahashi, "Terahertz time domain attenuated total reflection spectroscopy with an integrated prism system," *Rev. Sci. Instrum.*, vol. 83, no. 3, p. 033103, Mar. 2012.
[18] J. Wang, M. M. Kliks, S. Jun, M. Jackson, and Q. X. Li, "Rapid analysis of glucose, fructose, sucrose, and maltose in honeys from different geographic regions using Fourier transform infrared spectroscopy and multivariate analysis," *J. Food Sci.*, vol. 75, no. 2, pp. C208–14, Mar. 2010.
[19] S. Joly, F. Garet, J.-L. Coutaz, and M. Bernier, "Accurate determination of the complex refractive index of scattering materials by THz time-domain spectroscopy," in *Topical Meeting on THz Sci. Technol., Eur. Opt. Soc.*, Prague, Czech Republic, Jun. 2012.
[20] C. V. Raman and K. S. Viswanathan, "A generalized theory of the Christiansen experiment," *Proc. Indian Acad. Sci.*, vol. A41, pp. 55–60, Feb. 1955.
[21] R. Sardarly, O. Samedov, A. Abdullayev, F. Salmanov, A. Urbanovic, F. Garet, and J.-L. Coutaz, "Superionic conductivity in one-dimensional nanofibrous Tlgate2 crystals," *J. Appl. Phys.*, vol. 50, p. 05FC09, May 2011.

Maxime Bernier was born in France, in 1980. He received the M.Sc. degree in matter and radiation from the Burgundy University, France, in 2003, the M.Sc. degree in microwave and optical telecommunications from the University of Limoges, France, in 2004, and the Ph.D. degree in optic and radiofrequencies in 2008 from the Institut National Polytechnique of Grenoble (France) for a work dedicated to electro-optic detection of E-field.

He spent two years as a post-doctorate fellow within the laboratory of femtosecond spectroscopy at the University of Sherbrooke (Canada). Since September 2011, he is an assistant professor at the IMEP-LAHC laboratory, University of Savoy, where his activities are related to THz signal generation and detection, and accurate materials and devices characterization.

Frédéric Garet was born in France, in 1969. He received the Ph.D. degree in optics, optoelectronics and microwave from Institut National Polytechnique of Grenoble, France, in 1997.

From 1993 to 1997, he was involved in THz spectroscopy experiment at IMEP-LAHC Laboratory of the University of Savoy, France. Since 1998, he is an associate professor at IMEP-LAHC Laboratory. His current research interests the Terahertz Time Domain Spectroscopy field, and more precisely precise materials and devices characterization, thin films, THz optics, plasmonic, metamaterials.

Jean-Louis Coutaz received the Ph.D. degree from University of Grenoble, France, in 1981 and the "Docteur d'Etat" (habilitation) degree from the Technical University of Grenoble in 1987.

In 1981–1982, he was a lecturer at the University of Blida, Algeria, under a cooperation scheme. From 1983 to 1993, he was a full-time researcher at the French CNRS, working on guided wave nonlinear optics at INPG Grenoble. During 1988–1989, he was a postdoctoral fellow at the Royal Institute of Technology (KTH), Stockholm. In 1993, he became a professor of physics at the University of Savoie, where he has started research activities in ultrafast optoelectronics. Since 2007, he became the deputy director of the newly funded IMEP-LAHC, a common laboratory of CNRS, Grenoble INP, University Fourier of Grenoble and University of Savoie. He was a visiting professor at KTH Stockholm in 2000. His present research activities include THz-TDS, EO sampling and ultrafast III-V semiconductor devices.

Prof. Coutaz was the coordinator of several EC and NATO Science for Peace projects. Prof. Coutaz is a member of the French (SFO), European (EOS), and American (OSA) Optical Societies. He is a founding member of the EOS focus group on THz and of the International Society for Infrared, Millimeter and Terahertz Waves (Pasadena, CA, USA).